Research and Development Topics in Analytical Chemistry

The following are summaries of twenty of the papers and posters presented at a Meeting of the Analytical Division held on July 8th–9th, 1987, in the University of Strathclyde, Glasgow.

Application of Derivative Spectroscopy to the Alizarin Fluorine Blue - Lanthanum Determination of Fluoride

Marie M. Ferris, Brian Bingham and Michael A. Leonard
Department of Pure and Applied Chemistry, Queen's University, Belfast BT9 5AG

In dilute solution at pH 4.5, alizarin fluorine blue (1,2-dihydroxyanthraquinon-3-ylmethylamine-*N*,*N*-diacetic acid; AFB) is yellow ($\lambda_{max.}$ 423 nm), its lanthanum complex is red ($\lambda_{max.}$ 495 nm) and with fluoride ions this forms a blue ternary $(AFB)_2La_2F_2$ complex ($\lambda_{max.}$ 567 nm) instead of disintegrating to form AFB and LaF_3.[1,2] The spectral changes which occur on adding fluoride to $(AFB)_2La_2$ are illustrated in Fig. 1. This reaction has been used since 1958 as the basis of a specific absorptiometric analysis method for fluoride at about the 0.05 to 0.4 p.p.m. level. Fig. 2 shows spectra obtained when reagent - fluoride solutions are examined against a blank containing everything except fluoride; analytical measurements are usually made using the peak at 616 nm. In purely aqueous solution the calibration graph shows poorish linearity close to the origin which, when linear regression analysis is applied, yields an elevated detection limit. However, between

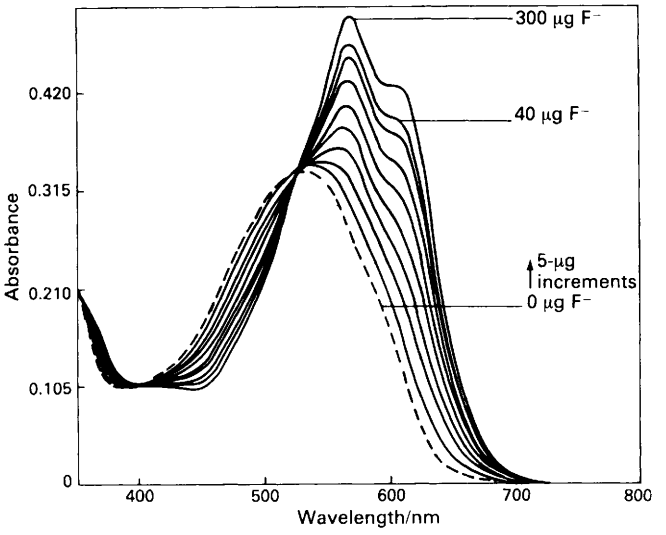

Fig. 1. Absorption spectra of AFB - La^{3+} solutions containing increasing amounts of fluoride. AFB = 5×10^{-5} M; La^{3+} = 5×10^{-5} M; pH = 4.6 (total acetate concentration about 0.06 M); solvent, 25% acetone; F^- concentration, 0.05–0.4 p.p.m. (also 3 p.p.m.); 1.0-m cell; slit width, 2.0 nm; scan speed, 960 nm min^{-1}. Blank is 25% acetone, pH 4.6

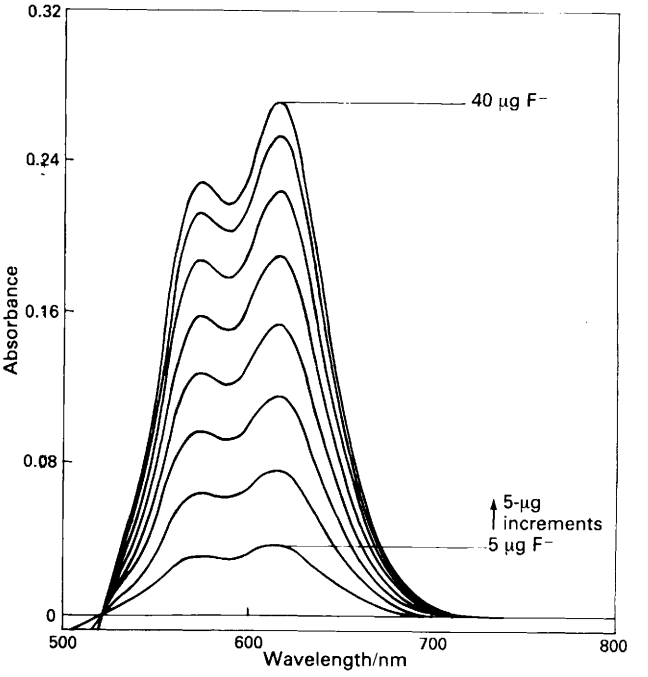

Fig. 2. Absorption spectra of AFB - La^{3+} solutions containing increasing amounts of fluoride measured against the full blank (all components except fluoride). Other conditions as for Fig. 1

Table 1. Calibration graph linear regression results: aqueous solutions

	Intercept, A or $dA/d\lambda$ or $d^2A/d\lambda^2$	Slope $dA/d\mu g$ per 100 cm^3, etc.	Correlation coefficient	No. of points	S.d. of pts about line A, $dA/d\lambda$, etc.	Lowest determinable X (μg per 100 cm^3 of F)
Absorption (low blank)	2.47×10^{-2}	2.47×10^{-3}	0.9944	9	3.85×10^{-3}	3.81
Absorption (high blank)	-6.86×10^{-3}	2.47×10^{-3}	0.9944	9	3.85×10^{-3}	3.80
First derivative (low blank)	-1.30×10^{-1}	7.89×10^{-3}	0.9916	6	1.08×10^{-2}	8.65
First derivative (high blank)	-3.20×10^{-2}	9.18×10^{-3}	0.9910	9	1.81×10^{-2}	4.71
Second derivative (low blank)	-2.61×10^{-3}	4.22×10^{-4}	0.9910	8	7.54×10^{-4}	5.68
Second derivative (high blank)	-1.52×10^{-3}	7.05×10^{-4}	0.9950	9	1.04×10^{-3}	3.60

Table 2. Calibration graph linear regression results: 25% acetone solutions

	Intercept, A or $dA/d\lambda$ or $d^2A/d\lambda^2$	Slope $dA/d\mu g$ per 100 cm^3, etc.	Correlation coefficient	No. of points	S.d. of pts about line A, $dA/d\lambda$, etc.	Lowest determinable X (μg per 100 cm^3 of F)
Absorption (low blank)	7.60×10^{-2}	6.43×10^{-3}	0.9989	8	4.00×10^{-3}	1.72
Absorption (high blank)	2.83×10^{-3}	7.39×10^{-3}	0.9992	8	3.91×10^{-3}	1.47
First derivative (low blank)	-1.21×10^{-1}	4.10×10^{-2}	0.9945	7	5.06×10^{-2}	4.55
First derivative (high blank)	-1.083×10^{-4}	4.66×10^{-2}	0.9991	8	2.68×10^{-2}	1.59
Second derivative (low blank)	-1.28×10^{-2}	3.38×10^{-3}	0.9970	7	3.13×10^{-3}	3.50
Second derivative (high blank)	1.89×10^{-3}	3.11×10^{-3}	0.9984	8	2.36×10^{-3}	2.08

10 and 30 μg of fluoride in 100 cm^3 linearity is good. Addition of acetone to about 25% improves both near-origin linearity and sensitivity but separation between the $(AFB)_2La_2$ and $(AFB)_2La_2F_2$ spectra diminishes.

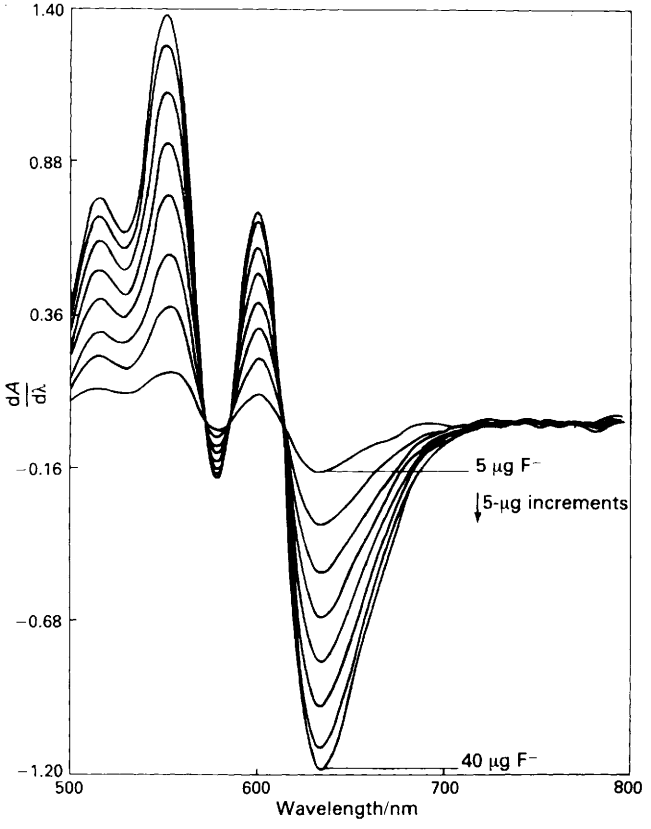

Fig. 3. First derivative spectra of AFB - La^{3+} solutions containing increasing amounts of fluoride measured against the full blank. Conditions as for Fig. 2 except for a scan speed of 120 nm min^{-1}; $\Delta\lambda$ = 10 nm

The availability of a Perkin-Elmer Lambda 9 ultraviolet - visible - near infrared spectrophotometer with excellent derivatising facilities led us to investigate whether working with derivative spectra ($dA/d\lambda$ and $d^2A/d\lambda^2$) would improve the fluoride analysis. The main feature of the first derivative of a Gaussian absorption band is a strong maximum followed by a strong minimum, with zero crossing coincident with $\lambda_{max.}$. The vertical distance between the peak and the trough is the amplitude and this is proportional to concentration provided that Beer's Law is obeyed in zero derivative. The second derivative spectrum is inverted with respect to the zero derivative and it features two satellite peaks flanking a strong minimum which corresponds to $\lambda_{max.}$. The vertical distance between the minimum and either the long or the short wavelength wing may be related to concentration. The valuable features of derivative spectra are the improvement of resolution between overlapping bands and the accentuation of "sharp" spectral features.[7,8] Fig. 2 shows the band width of the fluoride complex spectra to be comparatively small; hence, a derivative-based improvement seemed a reasonable possibility.

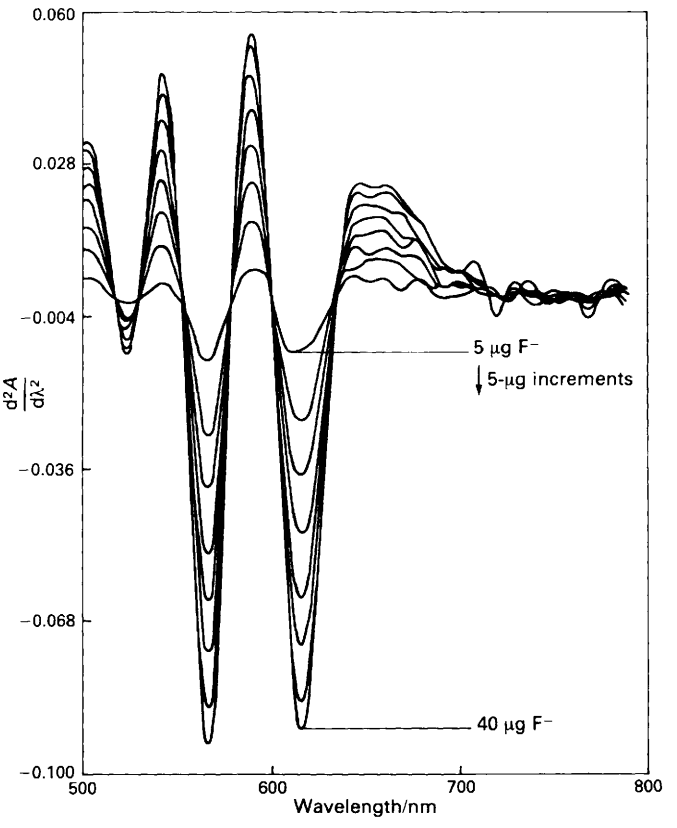

Fig. 4. Second derivative spectra of AFB - La^{3+} solutions containing increasing amounts of fluoride measured against the full blank. Conditions as for Fig. 3

Experimental

Stock solutions (5×10^{-4} M) of AFB and lanthanum nitrate were made up as described in references 1–6. A pH 4.6 buffer solution was prepared containing 150 g of hydrated sodium acetate and 75 cm^3 of glacial acetic acid per litre. Standard fluoride solution (5 μg cm^{-3}) was prepared from AnalaR or electronic grade sodium fluoride. Solutions for study contained 10 cm^3 of AFB, 10 cm^3 of La^{3+}, 3 cm^3 of buffer solution and 0–8 cm^3 of fluoride solution, made up to 100 cm^3 with the lanthanum added last. A 25-cm^3 volume of acetone can be included. More complete details can be found in references 1, 3 and 6. Purely aqueous solutions require 1 h to reach equilibrium, but the reaction in 25% acetone is much faster. Spectra were measured against either a blank containing buffer (and acetone) only or a full blank containing everything except fluoride.

Results

Fig. 3 shows the first derivative spectra of a series of solutions in 25% acetone plotted against the full blank. There is a clear isosbestic point at 615 nm, a positive peak at 602 nm and a negative peak at 635 nm; response was taken as the ordinate difference between the 602- and 635-nm peaks. The isosbestic point corresponds well with the higher $\lambda_{max.}$ of Fig. 2. Fig. 4 shows the 25% acetone full-blank second derivative spectra; these show good negative peaks at 565 and 615 nm. Measurements were taken between the 542 nm positive peak and the 565 nm negative peak. Table 1 shows linear regression results for the purely aqueous system and Table 2 those for the 25% acetone system. Points at high fluoride levels which obviously deviated from the line due to lack of reagent excess were excluded.

Conclusion

In purely aqueous solution there is little to choose between the various spectral derivatives; the lowest determinable mass of fluoride is disappointing in all instances. In 25% acetone solution "high blank" zero and first derivative analyses give equally good high-quality results; the second derivative is slightly inferior. Derivative "low blank" analyses are distinctly inferior. It is difficult to compare sensitivities when the ordinates are different but we feel that results from conventional 25% acetone high blank absorbance *versus* concentration graphs are not appreciably improved by derivatisation.

References

1. Leonard, M. A., and West, T. S., *J. Chem. Soc.*, 1959, 3577.
2. Langmyhr, F. J., Klausen, K. S., and Nouri-Nekoui, M. H., *Anal. Chim. Acta*, 1971, **57**, 341.
3. Belcher, R., and West, T. S., *Talanta*, 1961, **8**, 853.
4. Yamamura, S. S., Wade, M. A., and Sikes, J. H., *Anal. Chem.*, 1962, **34**, 1308.
5. Greenhalgh, R., and Riley, J. P., *Anal. Chim. Acta*, 1961, **25**, 179.
6. Leonard, M. A., *in* Johnson, W. C., *Editor*, "Organic Reagents for Metals and for Certain Radicals," Volume 2, Hopkin and Williams, Chadwell Heath, 1964, p. 1.
7. Cahill, J. E., *Am. Lab.*, 1979, **11**, 79.
8. Fell, A. F., *Proc. Anal. Div. Chem. Soc.*, 1978, **15**, 260.

Selective Fluorogenic Flow-injection Procedures for Primary, Secondary and Tertiary Amines in Non-aqueous Media

I. R. C. Whiteside and P. J. Worsfold
Department of Chemistry, University of Hull, Hull HU6 7RX

A. Lynes and E. H. McKerrell
Shell Research Ltd., Thornton Research Centre, P.O. Box 1, Chester CH1 3SH

Many compounds containing amine groups have useful industrial applications, *e.g.*, corrosion inhibitors, surfactants and biocides, and they are often formulated in oil-based matrices. Three non-aqueous flow-injection procedures with

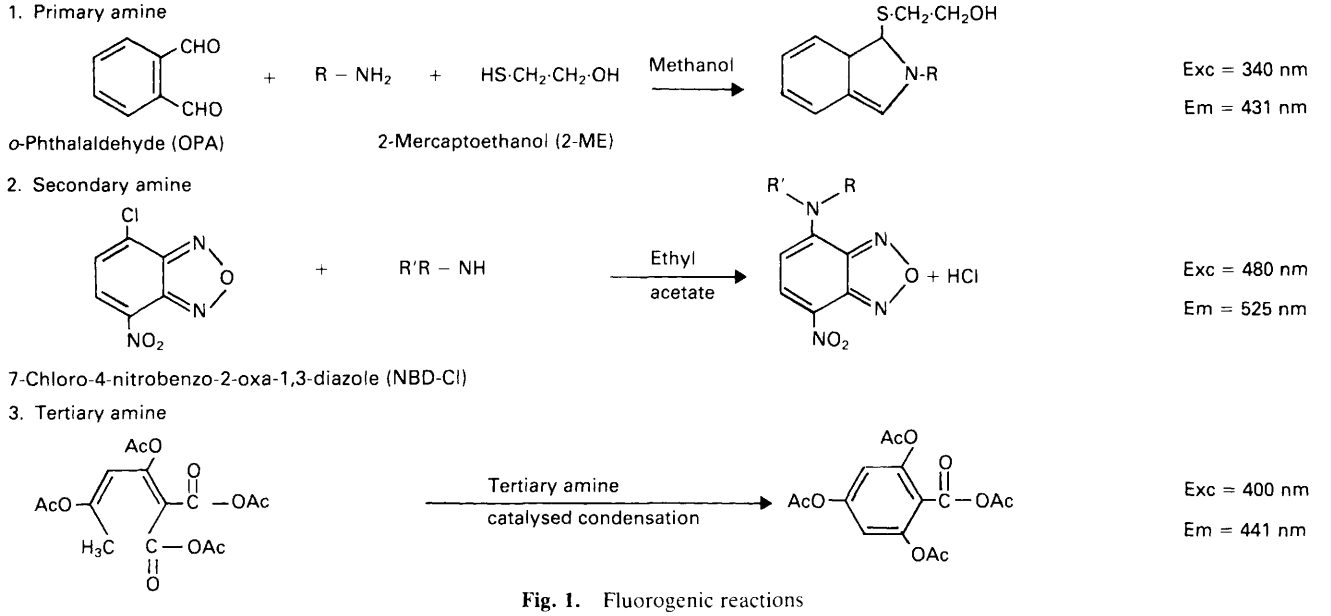

Fig. 1. Fluorogenic reactions

Table 1. Calibration data for hexylamine, dihexylamine and triethylamine

Functional group	Compound	Detection limit (2σ)/mM	Relative standard deviation ($n = 5$), %	Linear range/ mM
Primary amine	Hexylamine	0.04	1.0	0–0.8
Secondary amine	Dihexylamine	0.12	1.3	0–1.5
Tertiary amine	Triethylamine	0.005	2.1	0–2.5

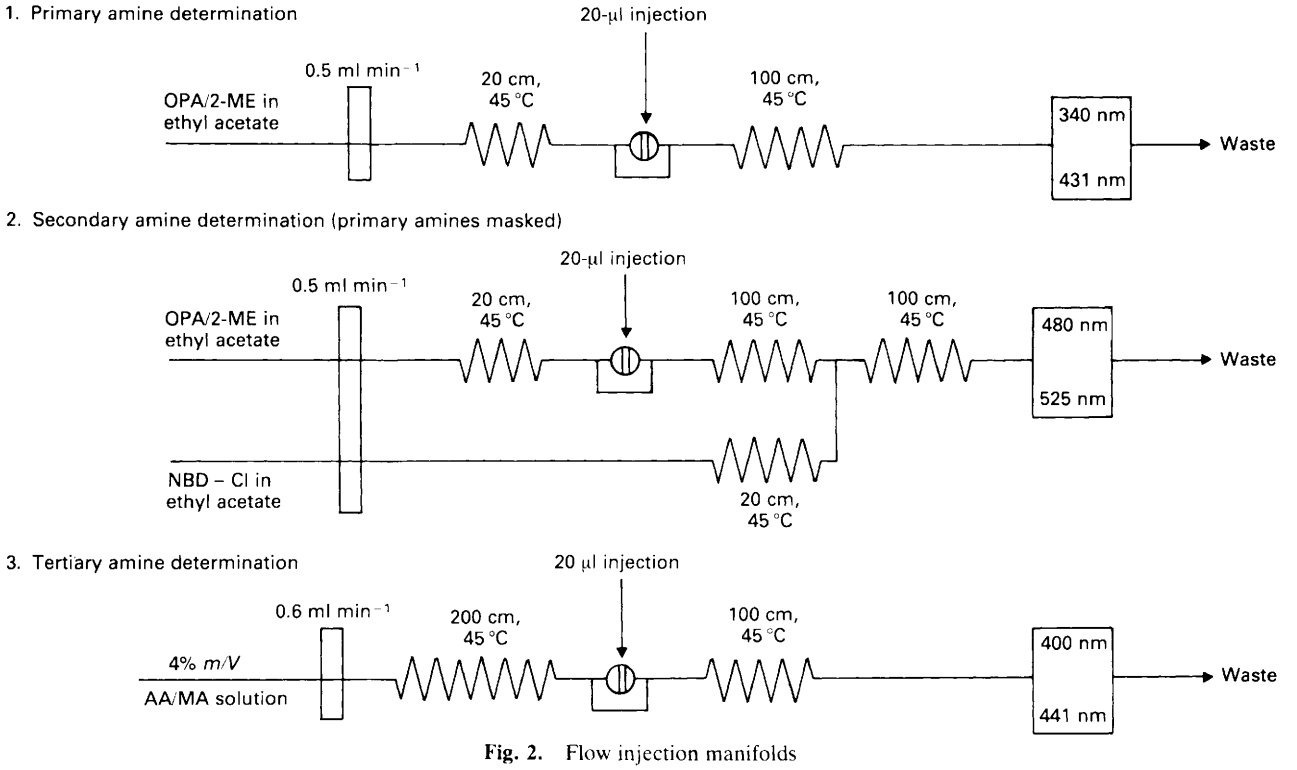

Fig. 2. Flow injection manifolds

fluorescence detection, selective for each of the amine functional groups (*i.e.* primary, secondary and tertiary) have been developed by using the reactions shown in Fig. 1.

Primary amines can be determined directly by derivatisation with *o*-phthalaldehyde(OPA) and 2-mercaptoethanol (2-ME) to form isoindole derivatives.[1] Secondary amines can be determined by derivatisation with 7-chloro-4-nitrobenzo-2-oxa-1,3-diazole (NBD-Cl) after on-line masking of primary amines by reaction with OPA/2-ME.[2] Tertiary amines can be determined by their ability to catalyse the cyclic condensation of malonic acid and acetic anhydride to form a fully acylated phloroglucinol carboxylic acid[3]; primary and secondary amines do not interfere because they form non-fluorescent *N*-substituted and *N*,*N*-disubstituted amides.

Experimental

The flow-injection manifolds used for the three procedures are shown in Fig. 2. For the determination of primary amines standards made up in ethyl acetate were injected into a single line carrier stream of OPA (58 mM) and 2-ME (58 mM) in ethyl acetate. For the determination of secondary amines standards made up in ethyl acetate were injected into a stream of OPA/2-ME (58 mM) and merged 100 cm downstream with NBD-Cl (28 mM) in ethyl acetate. For the determination of tertiary amines standards made up in tetrahydrofuran were injected into a single line carrier stream of malonic acid (4% *m*/*V*) in acetic anhydride. In all instances a 100 cm reaction coil at 45 °C was used and the detector was a fluorimeter (Perkin-Elmer LS-2) fitted with a 7 μl flow cell.

Results and Discussion

Calibration data for hexylamine, dihexylamine and triethylamine are given in Table 1, the results being typical of those obtained using low relative molecular mass aliphatic amines. The procedure for primary amines is specific, but the procedure for secondary amines is dependent on the capacity of the OPA/2-ME stream to remove primary amines prior to derivatisation with NBD-Cl, and this is affected by reagent concentration, reaction time and temperature. The procedure for tertiary amines is specific but primary and secondary amines can cause quenching of the fluorescence signals. These procedures could therefore be used to determine the total primary, secondary or tertiary amine content of a sample, but would need to be used in conjunction with HPLC for complete characterisation of a physical and chemical mixture of amines, and work is currently being done in this area.

The authors thank Thornton Research Centre, Shell Research Limited, for an Extra-Mural Research Grant in support of this work.

References

1. Simons, S. S., and Johnson, D. F., *J. Am. Chem. Soc.*, 1976, **98**, 7098.
2. Whiteside, I. R. C., Worsfold, P. J., and McKerrell, E., *Anal. Chim. Acta*, in the press.
3. Whiteside, I. R. C., Worsfold, P. J., and Lynes, A., *Anal. Chim. Acta*, 1987, **192**, 77.

Retention Modification in HPLC Using Metal Ions

Simon J. Bale and Roger M. Smith
Department of Chemistry, University of Technology, Loughborough, Leicestershire LE11 3TU

Stephen G. Westcott and M. Martin Smith
Glaxo Group Research, Ware, Hertfordshire SG12 0DJ

Metals are being used increasingly in HPLC as mobile phase additives to alter the selectivity of a separation. A number of methods have appeared in which a metal compound is incorporated in the mobile phase and is then adsorbed on to the silica surface of a reversed-phase packing.[1,2] This alters the selectivity by changing the polar, steric and solvation properties of the stationary phase. Another technique has involved the addition of chiral metal compounds, usually amino acid complexes, to the mobile phase to facilitate enantiomeric separations.[3,4] A method which has seen little utilisation to date is the use of simple metal salts as mobile phase modifiers, such as zinc chloride[5] and nickel acetate.[6]

In many instances the role played by the metal ions in these separations has not been fully established. We have recently investigated the effect of a range of metal ions on the retention of 2-aminophenol.[7] This was used as a model compound, to give a more detailed understanding of the retention modification caused by simple transition metal ions in the mobile phase. It was found that all of the metals studied caused a reduction in retention, owing to the formation of a more polar species with the metal ions, and that the size of the reduction was dependent on the metal ion concentration. The pH of the mobile phase was also shown to be an important factor, and in general, increasing the pH increased the size of the effect of the metal ions. The metals studied had effect in the order

$$Cu > Ni > Co > Zn > Cd > Mn$$

This work has now been extended to take into account the various equilibria present in solution and a theoretical model has been developed to explain the variation in retention of 2-aminophenol with metal ions in the mobile phase.

Experimental

The chromatography was performed by using a Pye Unicam PU4010 pump, a Rheodyne 7125 injection valve fitted with a 20 μl sample loop and a Pye Unicam PU4020 variable wavelength detector set at 280 nm. The retention of 2-aminophenol (20-μl injections, 10^{-3} M) was studied using a porous polystyrenedivinylbenzene polymer column (PLRP-S, 100 mm × 5 mm) thermostatted at 30 °C using a water jacket. Aqueous mobile phases (10, 20 and 30% methanol), containing 0.26 M ammonium acetate and low levels of transition metal acetates, were used at a flow-rate of 1 ml min^{-1}. The pH of the mobile phase (6, 7.24 or 8) was adjusted by use of concentrated hydrochloric acid or sodium hydroxide solution.

Discussion

In aqueous solution, and in the absence of metal ions, 2-aminophenol is present in three forms: the protonated amino cation (AH_2^+), the neutral molecule (AH) and the phenolate anion (A^-). The relative proportions of these species are pH dependent, and the equilibria between the three forms are governed by the pK_a values of the amine and phenol groups, K_{a_1} and K_{a_2}.

In the presence of metal ions the phenolate anion forms chelates and two further species may be introduced into the equilibrium, the 1:1 (MA^+) and 2:1 (MA_2) chelates. The proportions of these two species are dependent on their formation constants K_1 and K_2.

When 2-aminophenol is injected on to an HPLC column and eluted with an eluent containing metal ions the same equilibria as above are set up, and these are, in turn, in equilibrium with the stationary phase:

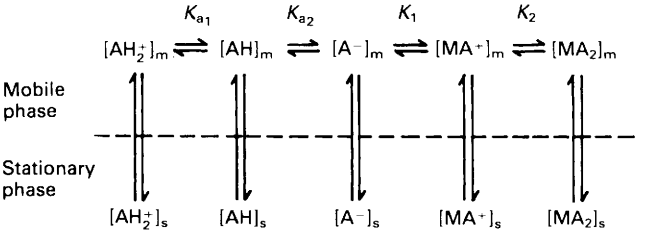

The capacity factor (k') for the over-all system can be defined as

$$k' = \frac{\text{Amount in stationary phase}}{\text{Amount in mobile phase}}$$

$$= \frac{q[AH^+_2]_s + [AH]_s + [A^-]_s + [MA^+]_s + [MA_2]_s}{[AH^+_2]_m + [AH]_m + [A^-]_m + [MA^+]_m + [MA_2]_m}$$

where q = phase ratio. Each of the five species has a capacity factor: k'_b for the protonated amine, k'_n the neutral molecule, k'_i the phenolate anion, k'_{c_1} the 1:1 chelate and k'_{c_2} the 2:1 chelate.

If substitutions are made for the equilibrium concentrations and stationary phase terms, the following equation is obtained:

$$k' = \frac{k'_n + \dfrac{k'_b[H^+]}{K_{a_1}} + \dfrac{k'_i K_{a_2}}{[H^+]} + \dfrac{k'_{c_1} K_1 K_{a_2}[M^{2+}]}{[H^+]} + \dfrac{k'_{c_2} K_1 K_2 K_{a_2}[M^{2+}][A^-]}{[H^+]}}{1 + \dfrac{[H^+]}{K_{a_1}} + \dfrac{K_{a_2}}{[H^+]} + \dfrac{K_1 K_{a_2}[M^{2+}]}{[H^+]} + \dfrac{K_1 K_2 K_{a_2}[M^{2+}][A^-]}{[H^+]}}$$

This equation contains a term for 2:1 chelate formation involving the free ligand concentration $[A^-]$. This suggests that the capacity factor of 2-aminophenol, and in general the analyte, is concentration dependent. However, because the metal ions present in the mobile phase are in vast excess (between 0.02 and 0.4 M compared with 0.000 1 M analyte at pH 7.24), and 2:1 chelate formation depends overall on the free ligand concentration $[A^-]^2$, only very small amounts of the 2:1 chelate are formed with the injection concentrations used in HPLC. Chelate formation tends to the formation of MA^+ as

the metal ion concentration increases and the equation for capacity factor can be reduced to

$$k' = \frac{k'_n + \frac{k'_b[H^+]}{K_{a_1}} + \frac{k'_i K_{a_2}}{[H^+]} + \frac{k'_{c_1} K_1 K_{a_2}[M^{2+}]}{[H^+]}}{1 + \frac{[H^+]}{K_{a_1}} + \frac{K_{a_2}}{[H^+]} + \frac{K_1 K_{a_2}[M^{2+}]}{[H^+]}}$$

At very low concentrations, when the ligand is in excess, competition with protons dominates the expression and insufficient ligand becomes available for 2:1 chelate formation. In the absence of metal ions this equation reduces still further to give an equation describing the variation of the capacity factor of an ampholyte with pH; this form contains the two expressions derived by Miyake[8] *et al.* for the capacity factor of an acidic and a basic compound.

The variation of capacity factor with metal ion concentration at constant pH was tested using the expression

$$k' = \frac{a + b[M^{2+}]}{1 + c[M^{2+}]}$$

where a, b and c are constants related to those above. If the pK_a values of the groups are known then all the other capacity factor terms and formation constants can be determined from a, b and c.

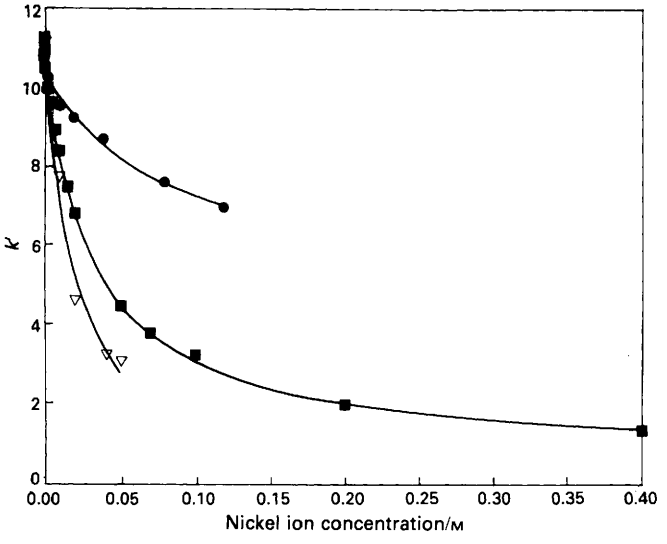

Fig. 1. Graphs showing the correlation for the effect of the presence of nickel ions on the capacity factors of 2-aminophenol, between the experimental values at pH 6 (●), pH 7.24 (■) and pH 8 (▽), and the corresponding calculated values depicted by the solid lines

This expression was fitted to experimental data by using a non-linear least squares computer program (Genstat 4.03). High coefficients of correlation have been obtained and the same constants have been obtained under a variety of experimental conditions.

The formation constant of the 1:1 chelate of 2-aminophenol with nickel ions was determined by using the equations derived above with experimental data obtained at pH 6, pH 7.24 and pH 8 (Fig. 1). The formation constants found in this way were $\log_{10}K_1$ 4.2 (pH 6), 4.67 (pH 7.24) and 4.85 (pH 8). These constants were calculated by using a pK_a value of 10.43 for the phenol group, which had been previously determined by spectroscopy, and by HPLC using the relationship between capacity factor and pH.

While very good correlations have been obtained for fitted and experimental data the accuracy of the calculated formation constants requires an accurate determination of k'_{c_1}, the capacity factor of the 1:1 chelate. This often requires the use of very high concentrations of metal ions in the mobile phase, more than 0.5 M, which poses problems for the detection background, and adjustment of the pH.

Conclusion

The addition of metal ions in the mobile phase is a technique which may be used to alter the selectivity of a separation. Analytes that are capable of chelation can be made to form polar species with metal ions and their retention times are reduced. The influence that a given metal may have is dependent on the magnitude of its chelate formation constant with the analyte, its concentration and the mobile phase pH.

A model has been proposed for the behaviour of 2-aminophenol in mobile phases containing metal ions which accurately describes experimental measurements. This model may be useful in predicting the effect of metal ions in the mobile phase on the chromatography of other chelating analytes.

References

1. Lochmuller, C. H., and Hangac, H. H., *J. Chromatogr. Sci.*, 1982, **20**, 171.
2. Cooke, N. H. C., Viviattene, R. L. R., Eksteen, R., Wong, W. S., Davies, G., and Karger, B. L., *J. Chromatogr.*, 1978, **149**, 391.
3. Le Page, J. N., Lindner, W., Davies, G., Seitz, D. E., and Karger, B. L., *Anal. Chem.*, 1979, **51**, 433.
4. Gilon, C., Leshem, R., Tapuli, Y., and Grushka, E., *J. Am. Chem. Soc.*, 1979, **101**, 7612.
5. Walters, V., and Raghaven, N. V., *J. Chromatogr.*, 1979, **176**, 470.
6. Sternson, L. A., Dixit, A. S., Riley, C. M., Siegler, R. W., and Schoech, D., *J. Pharm. Biomed. Anal.*, 1983, **1**, 105.
7. Smith, R. M., Bale, S. J., Westcott, S. G., and Martin-Smith, M., *Analyst*, 1987, **112**, 1209.
8. Miyake, K., Okrumura, K., and Terada, H., *Chem. Pharm. Bull.*, 1985, **33**, 769.

HPLC Determination of Trace Metals in Industrial and Environmental Samples

Mary Meaney, Joseph Mooney, Michelle Connor and Malcolm R. Smyth
School of Chemical Sciences, NIHE Dublin, Glasnevin, Dublin 9, Ireland

The determination of trace metals using HPLC-based technology has received much attention in recent years.[1–6] The main reasons for this stem from the possibilities firstly of having a multi-element technique using equipment that is now commonly available in most laboratories and which need not be dedicated solely to this application, and secondly, of obtaining information on the "speciation" of a certain element in a certain matrix.

To date, we have investigated the application of reversed phase HPLC to the determination of trace concentrations of copper(II) and iron(III) in anaerobic adhesives,[7] and the levels of iron(III) and aluminium(III) in soil and clay samples following a variety of sample extraction procedures.[8]

The determination of trace metal concentrations by HPLC is based on the assumed quantitative formation of a stable metal chelate *in situ*. The metal ion of interest can be introduced on to

the column either by "direct injection" of the metal ion in its ionic form, or by injection of a solution of the metal chelate formed "externally" using the same ligand that is employed in the chromatographic eluent. By using the "direct injection" technique, limits of detection in the low p.p.m. range can usually be achieved. Much lower limits of detection (of the order of 50 p.p.b.) can, however, be achieved following external formation of the metal chelate, assuming that the background metal ion concentration is of the order of 10 p.p.b. This is illustrated for the case of iron(III) in Fig. 1.

In the optimisation of an HPLC method for the determination of a certain metal ion, the following parameters are of importance.

1. *Ligand concentration*. The optimum ligand concentration should be investigated bearing in mind the range of metal ion concentrations to be determined, and should be the concentration which gives rise to the largest and most stable absorbance reading (relating to the chelate) in the shortest time possible.

2. *pH*. The acid - base equilibria of the ligand should be investigated in order to optimise conditions for chelate formation: again, the absorbance readings obtained for the chelate under different conditions of pH should reflect the largest and most stable readings in unit time.

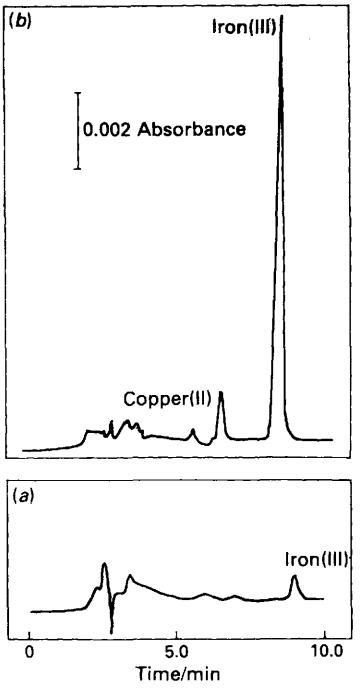

Fig. 1. Comparison of HPLC chromatograms for the determination of iron(III) following (*a*) "*in situ*" formation of iron(III) - oxine complex, and (*b*) external formation of the iron(III) - oxine complex

3. *Solvent composition*. The ratio of aqueous to organic solvent should be varied to investigate the stability of the chelate under the conditions that are generally employed for HPLC separations, *e.g.*, the copper(II) - oxine chelate has been found to be unstable at aqueous buffer: acetonitrile ratios of greater than 50:50, and hence these ratios cannot be used for HPLC separations involving this metal chelate.[7]

4. *Salt concentration*. In some instances it has been reported that metal chelates can be stabilised by the addition of a salt to the mobile phase, *e.g.*, the addition of potassium nitrate to the mobile phase was advocated by Bond and Nagaosa[6] for stabilisation of the iron(III) - oxine chelate.

5. *Detection wavelength*. The detection wavelength should be optimised with respect to the absorption maximum of the chelate and the background absorbance due to the mobile phase of choice.

6. *Column selection*. It has been our experience that the best separations of metal chelates is achieved on columns which have been "end-capped" to prevent free SiOH groups on the stationary phase interfering in the separation.

The number of metal ions which can be determined simultaneously by using this approach can be of the order of five or six, but this depends to a large extent on the choice of ligand, the operating conditions and the matrix involved. The ligands investigated to date include dithiocarbamates, β-diketonates, Schiff bases, dithizone, crown ethers, etc. In our studies, we have concentrated on the use of oxine as a ligand because of: firstly, the separation that one can achieve, especially with respect to copper(II) - and iron(III) - oxinates; and secondly, the ability to use this compound as an extractant of metal ions from complex matrices such as soils and clays. The HPLC approach to trace metal analysis can therefore be useful in situations where a large number of metal ions (particularly transition metal ions) need to be determined in a short space of time or as a complementary method to atomic absorption spectroscopy (AAS) or anodic stripping voltammetry (ASV) when the results of two independent methods are required.

The information that one obtains from HPLC determinations of this kind does not necessarily correlate with that obtained from AAS, however, as this approach is primarily geared to looking at the "free" or "available" metal ion concentration rather than the "total" metal ion concentration. This has been demonstrated in our studies both on the anaerobic adhesives[7] and on the soil and clay samples.[8] In the former study, anaerobic adhesive formulations were investigated which contained 300–400 p.p.m. of EDTA. In these formulations, however, EDTA is only present in the "soluble" form to the extent of approximately 20 p.p.m. and the HPLC method developed could only detect concentrations of copper(II) and iron(III) spiked into the formulations when this concentration limit was exceeded. In the instances of soil and clay samples discrepancies have been noticed in the concentrations of aluminium(III) extracted under various conditions and determined separately by HPLC and AAS. The AAS results were consistently higher than those obtained by using HPLC and the difference in these results would appear to be due to "bound" aluminium(III) species co-extracted with the "free" portion.

This ability of HPLC to speciate between "free" and "bound" metal ions in environmental and industrial samples, coupled perhaps with electrochemical detection, should prove of major interest in the near future.

References

1. Bond, A. M., and Wallace, G. G., *Anal. Chem.*, 1982, **54**, 1706.
2. Smith, R. M., Butt, A. M., and Thakur, A., *Analyst*, 1985, **110**, 35.
3. Inatimi, E., *J. Chromatogr.*, 1983, **256**, 256.
4. Guira, R. C., and Carr, P. W., *J. Chromatogr. Sci.*, 1982, **20**, 10.
5. O'Laughlin, J. W., and Hanson, R. S., *Anal. Chem.*, 1982, **54**, 178.
6. Bond, A. M., and Nagaosa, Y., *Anal. Chim. Acta*, 1985, **178**, 197.
7. Mooney, J., Meaney, M., Leonard, R., Wallace, G. G., and Smyth, M. R., *Analyst*, 1987, **112**, 1555.
8. Meaney, M., Connor, M., Breen, C., and Smyth, M. R., in preparation.

Ion Exchange Resin and Soil Solution Measurements of Soil Potassium and its Uptake by Ryegrass and Clover

G. D. Wimaladasa* and A. H. Sinclair†
Department of Soil Fertility, The Macaulay Land Use Research Institute, Craigiebuckler, Aberdeen AB9 2QJ

There is no universal agreement on the best methods for extracting soil solution or non-exchangeable soil potassium. A centrifugal method for extracting soil solution for the determination of potassium and a mixed ammonium chloride - ion exchange resin procedure for extracting both exchangeable and non-exchangeable potassium are described.

Introduction

Soil potassium occurs notionally in four different forms that are in equilibrium with each other, but differ in their availability to plants.

$$\text{Mineral K} \overset{\text{III}}{\rightleftharpoons} \text{Non-exchangeable K} \overset{\text{II}}{\rightleftharpoons} \text{Exchangeable K} \overset{\text{I}}{\rightleftharpoons} \text{Soil Solution K}$$

Potassium release to plants in a single growing season is dominated by equilibrium I, whereas II and III affect the long-term availability.[1] Plants obtain their nutrients largely, if not exclusively, by uptake from solution in soil.[2] However, little attention has been paid to the seasonal variations in K concentration in the soil solution and its relationship with the soil solid phases. There are various reasons for this. Soil solution has been regarded as difficult to obtain in a form likely to relate closely to that present in undisturbed soil. Numerous methods have been proposed either to isolate soil solution, such as liquid displacement and lysimeters, or to estimate potassium in soil solution, such as electro-ultrafiltration (EUF) and quantity/intensity measurements, but none has proved entirely satisfactory.[2-4] In this paper we describe a modified centrifugal method of isolating soil solution and the behaviour of K^+ in soil solution within the rooting zone of ryegrass in the field.

An assessment of the rate of replenishment of potassium in the soil solution from the solid phase is required in order to understand soil - plant - potassium interactions. Numerous methods have been used to measure the concurrent release of non-exchangeable potassium together with exchangeable potassium during the growing season.[5-7] In this paper a novel method involving NH_4^+-ion exchange resin has been used to study the chemistry of soil potassium dynamics and the results have been compared with standard methods.

Materials and Methods

Soil Solution

Soil solutions were isolated by centrifugation of 300 g of field moist soil at 3000 × *g* for 60 min in a two-component cell (diameter 9 cm and total height 10 cm) separated by a perforated disc.[8] Whatman No. 42 filter-paper was placed on the perforated disc and disposable polythene bags were used to reduce the possible contamination of the soil solution. The solution collected in the lower part of the cell was separated and re-filtered through a Whatman No. 42 filter-paper to avoid contamination due to fine clay material. Potassium concentrations were determined by flame photometry.

When the soil samples were too dry to allow collection of enough solution for chemical analyses, samples were re-moistened by adding de-ionised water up to 90% of the field capacity. Re-moistened soil samples were stored in the cold room for 3–4 d and thoroughly mixed. Forty-eight soil samples can be centrifuged per day provided that the centrifuge has a six-component head with appropriate dimensions equivalent to the cell.

Mixed Ammonium-Cation Exchange Resin and Chloride-Anion Exchange Resin Preparation

Four grams of Duolite 225 H resin (BDH, particle size of 0.50–1.18 mm) and 4.0 g of Amberlite Cl-resin (BDH, IRA-400, particle size of 0.30–1.18 mm) were introduced into a nylon netting bag (3.5 × 6.5 cm) with a mesh size of 0.2 mm. The oblong and tetrahedron shaped bags were sealed by means of an electric sealer.[9] These mixed-resin bags were equilibrated with excess of 1 M ammonium chloride and 0.0 1 M hydrochloric acid (1 : 1) solution in an orbital shaker. After the equilibration the pH of the solution was measured and a fresh solution of 1 M NH_4Cl and 0.01 M HCl was introduced. This procedure was repeated until the pH was constant. The excess ions were washed free in the same vessel with de-ionised water until the chloride ion concentration dropped to a minimum. The final resin material contained NH_4^+ and Cl^- ions. Resin bags were stored under de-ionised water in order to avoid breakdown of the resin beads.

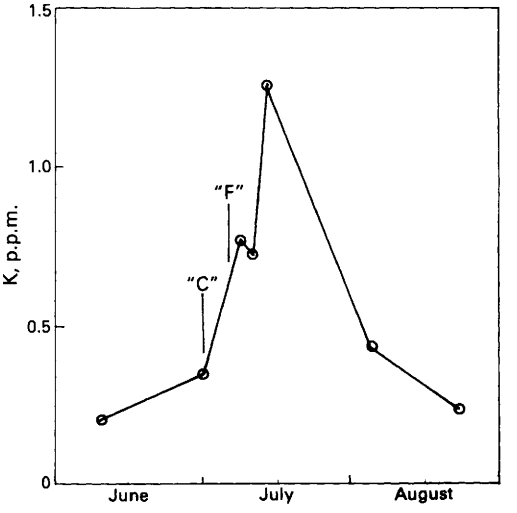

Fig. 1. Potassium concentrations (p.p.m.) in soil solutions from treatment N_2K_0 where "C" is the time of grass cutting and "F" is the time of fertiliser addition

Soil Potassium Extraction With Ammonium Chloride - Ion Exchange Resin

Air-dried soil, equivalent to 5.0 g of oven-dried soil, which had been passed through a 2-mm sieve, was equilibrated with 100 ml of de-ionised water and a mixed-resin bag in a wide mouth polypropylene bottle for 16 h (overnight) held in an end-over-end shaker. After the equilibration, the ion exchange resin bags were removed from the soil - water suspension and washed thoroughly with de-ionised water. The resin bags were eluted with 100 ml of 1 M NH_4Cl and 0.01 M HCl (1 + 1) solution for 30 min and the potassium concentration was measured by flame photometry.

* Home Address: Tea Research Institute of Sri Lanka, Talawakelle, Sri Lanka.
† Present Address: The North of Scotland College of Agriculture, Aberdeen.

Table 1. Correlation coefficients of linear regressions of exchangeable and resin extractable soil potassium on cumulative potassium uptake and quadratic regressions on yield of ryegrass at different cropping stages

	K uptake at cut no.			Yield at cut no.		
K measurement	1	1 + 2	1 + 2 + 3	1	1 + 2	1 + 2 + 3
1 M NH_4OAc (K_{ex})	0.928	0.981	0.981	0.682	0.869	0.934
Mixed NH_4Cl - ion exchange resin (K_r) (all $P < 0.001$)	0.943	0.982	0.980	0.642	0.845	0.917

Nitrification of NH_4-Ion Exchange Resin

The possibility of nitrification of NH_4-ion exchange resin material during the 16-h equilibration with soil - water suspension was studied by using "Nitrapyrin" [2-chloro-6-(trichloromethyl)pyridine] as a nitrification inhibitor.[10] Three soils of different pH values (4.0, 4.8 and 5.5) were equilibrated with 4.0 g of the ammonium-cation exchange resin and 100 ml of de-ionised water for 16 h with and without the presence of 15 μg ml^{-1} "Nitrapyrin." A control set of soils were equilibrated without resin bags. After the equilibration, the soil suspensions were filtered through Whatman No. 42 filter-paper. The nitrate concentration in the filtrate was measured colorimetrically after reduction to nitrite with hydrazine (Industrial Method No: 333-86E, Technicon).

Results and Discussion

Soil Solution Potassium

A ryegrass and clover field experiment (Countesswells soil series)[11] with and without fertiliser potassium was selected to monitor the concentration of potassium in soil solutions within the rooting zone soil. Soil solution potassium levels were in the range of 0.20–1.26 p.p.m. in the plots with zero potassium applied and 0.50–4.38 p.p.m. in the plots receiving 70 kg ha^{-1} cut^{-1} of potassium as potassium chloride. The nitrogen addition to all plots was 110 kg ha^{-1} cut^{-1} as ammonium nitrate. Soil samples were collected at 2-week intervals except immediately after fertiliser application, when sampling was at 2-d intervals.

Fig. 1 gives the variation of soil solution potassium levels. The letter "C" indicates when the sward was cut and "F" indicates the timing of ammonium nitrate application. The increase in soil solution potassium concentration following the addition of nitrogen fertiliser alone (N_2K_0) is attributed to displacement of K^+ from exchange sites by NH_4^+ from the fertiliser. This finding has implications in fertiliser use.

Mixed Ammonium Chloride - Ion Exchange Resin Potassium

Potassium was extracted from 41 soil samples with the mixed ammonium chloride - ion exchange resin (K_r) and the results compared with yield and crop potassium uptake from these soils by ryegrass grown in pots, and with potassium extracted by the conventional method using 1 M ammonium acetate solution at pH 7.0 (K_{ex}).[3]

The K_r results in Table 1 show similar linear correlations between soil test value and K uptake by ryegrass compared with conventional K_{ex}. An additional advantage of the mixed ammonium chloride - ion exchange resin is its ability to extract available soil phosphorus.[12] Loosely held, non-exchangeable K, K_{int}, is not extracted by 1 M ammonium acetate solution, but becomes available to ryegrass. A close correlation between K_{int} and K_{ex} has been shown,[1] which helps to explain the observed close correlations between K_{ex} and ryegrass data. However, the mixed ammonium chloride - ion exchange resin does extract part of the non-exchangeable K. This ability to extract non-exchangeable K is demonstrated by the relationship

$$K_r = 0.674\ K_{ex} + 0.935,\ r = 0.986\ (P < 0.001)$$

The equation shows that the greatest proportion of non-exchangeable K, compared with exchangeable K, is extracted by the ion exchange resin from soils of low exchangeable K. The rate of release of this non-exchangeable K is being investigated by means of sequential ion exchange resin extractions.

A quadratic relationship was found between the yield of ryegrass and soil K values (Table 1).

Nitrification of Ammonium-Ion Exchange Resin

The nitrate concentrations in Table 2 indicate that nitrification of ammonium-ion exchange resin was not significant during the 16-h period.

Table 2. Nitrate-nitrogen concentrations (p.p.m.) in aqueous extracts of soil with and without the presence of ammonium-ion exchange resin and nitrapyrin

	Soil pH		
Extractant	4.0	4.8	5.5
Soil - water	0.52	0.91	2.25
Soil - water - NH_4^+-ion exchange resin	0.55	0.86	1.60
Soil - water - NH_4^+-ion exchange resin - nitrapyrin	0.54	0.72	1.53
Standard error of means = ±0.047			

Conclusion

The proposed centrifugal and mixed ammonium chloride - ion exchange resin techniques have proved useful for measuring the K concentration in soil solution and its replenishment from exchangeable and non-exchangeable sources as part of a wider study of soil - plant - potassium dynamics.

We wish to thank Dr. D. Atkinson and members of the Departments of Soil Fertility, Spectrochemistry, Statistics and Technical Services for their assistance. G. D. Wimaladasa wishes to thank the Director, Tea Research Institute of Sri Lanka, for financial assistance and study leave.

References

1. Sinclair, A. H., *J. Soil Sci.*, 1979, **30**, 757.
2. Adams, F., Burmester, C., Hue, N. V., and Long, F. L., *Soil Sci. Soc. Am. J.*, 1980, **44**, 733.
3. Sinclair, A. H., *Plant Soil*, 1982, **64**, 85.
4. Ghorayshi, M., and Lotse, E. G., *Swedish J. Agric. Res.*, 1986, **16**, 143.
5. Sinclair, A. H., *J. Soil Sci.*, 1979, **30**, 775.
6. Salomon, M., and Smith, J. B., *Soil Sci. Soc. Proc.*, 1957, **21**, 222.
7. Arnold, P. W., *Nature*, 1958, **182**, 1594.
8. Linehan, D. J., Sinclair, A. H., and Mitchell, M. C., *Plant Soil*, 1985, **86**, 147.
9. Sibbesson, E., *Plant Soil*, 1977, **46**, 665.
10. Powell, S. J., and Prosser, J. I., *App. Environ. Microbiology*, 1986, **52**, 782.

11. Glentworth, R., and Muir, J. W., "The Soils of the Country Around Aberdeen, Inverurie and Fraserburgh. Memoirs of the Soil Survey of Scotland. Edinburgh," HM Stationery Office, Edinburgh, 1963.

12. "The Macaulay Institute for Soil Research, Annual Report," Volume 56, Macaulay Institute for Soil Research, Aberdeen, 1986, p. 183.

On-line Pre-concentration with a Boron-specific Resin in Flow Injection - Inductively Coupled Plasma Emission Spectrometry

D. R. Anderson and C. W. McLeod
Department of Metals and Materials Engineering, Sheffield City Polytechnic, Sheffield S1 1WB

Recent studies in our laboratories have demonstrated the usefulness of activated alumina for on-line trace enrichment of a wide range of cations and anions, including phosphate, chromate and sulphate.[1] This approach, however, was relatively unsuccessful for borate, on account of poor analyte retention characteristics.

Given the need for improving current methodology for the determination of boron in complex samples, an alternative column packing was sought. Thus, a boron-specific resin was utilised in the present study.

Experimental

The flow injection manifold and ICP instrumentation have been described elsewhere.[2] The microcolumn (1.5 × 50 mm) was packed with Amberlite XA743 (Rohm and Haas) of particle size range 180–420 μm. Experimental parameters were: carrier stream flow-rate (distilled water), 0.75 ml min^{-1}; sample volume, 250 μl; eluent, nitric acid (1 M, 250 μl). Plasma operating conditions were: forward power, 1.1 kW; coolant argon flow, 17 l min^{-1}; nebuliser argon flow, 0.7 l min^{-1}; analytical wavelength, 249.77 nm. Standard solutions were prepared from BDH chemicals (Spectrosol). A synthetic steel sample was prepared (iron 1000 μg ml^{-1}, boron 1 μg ml^{-1}, pH 3.0) and EDTA added to prevent iron precipitation.

In the procedure, boron was deposited on the column either by injection (250 μl), or by pumping the sample for specified time periods, *e.g.*, 2 min. Elution was subsequently effected by injection of nitric acid (250 μl); the signal was measured either as an emission - time profile or an integrated peak area.

Results and Discussion

A typical emission time response for the deposition - elution sequence is shown in Fig. 1. For the experimental parameters given, and for column lengths greater than 5 cm, it was established that more than 90% of analyte was deposited for samples of pH 3–10, and that nitric acid (1 M, 250 μl) was an effective eluent. For column lengths less than 5 cm, deposition efficiency was impaired.

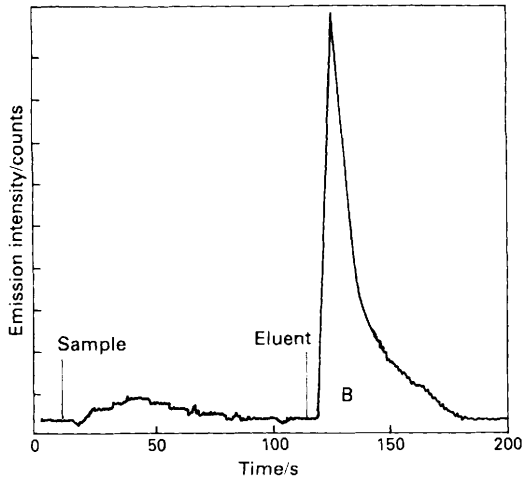

Fig. 1. The deposition - elution sequence: sample boron, 1 μg ml^{-1}

A scheme for the deposition - elution process, analogous to the boric acid - mannitol reaction, is:

$$B(OH)_3 \rightleftharpoons B(OH)_4^- \overset{H^+}{\rightleftharpoons} R\text{-}B(OH)_2$$

Resin - borate complex

At pH values above 3 and in the presence of the resin, complexation takes place and the equilibrium is shifted to the right. Upon addition of acid, the boron species reverts to boric acid.

A calibration graph, based on the injection of samples, was established over the concentration range from 10 μg l^{-1} to 100 μg ml^{-1}, and this revealed a significant breakthrough of analyte at concentrations above 20 μg ml^{-1}. The breakthrough capacity for boron at this point was estimated to be 23 μg per gram of resin. The use of larger sample injection volumes gave enhanced sensitivity. The relative standard deviation for seven replicates at 100 μg l^{-1} was 1.5%.

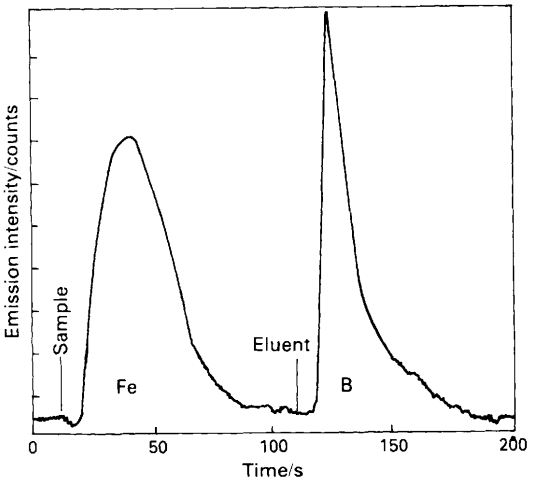

Fig. 2. The deposition - elution sequence: sample boron, 1 μg ml^{-1}, iron, 1000 μg ml^{-1}

The matrix removal capability of the flow injection manifold was investigated with respect to iron, because it is well known that the determination of boron in steels by ICP-AES is subject to spectral interference.[3] A synthetic steel sample (iron 1000 μg ml^{-1}, boron 1 μg ml^{-1}) was injected (250 μl) into the manifold and the response is shown in Fig. 2. This reveals the time resolved emission responses for iron and boron. Work is currently in progress on the determination of boron in complex matrices.

References

1. McLeod, C. W., *J. At. Spectrom.*, 1987, **2**, 549.
2. McLeod, C. W., Cook, I. G., Worsfold, P. J., Davies, J. E., and Queay, J., *Spectrochim. Acta, Part B*, 1985, **40**, 57.
3. Wallace, G. F., *At. Spectrosc.*, 1981, **2**, 61.

Laser Ablation for the Mobilisation of Refractory Materials in Analytical Atomic Spectroscopy

Simon Chenery
Applied Geochemistry Research Group, Department of Geology, Imperial College, South Kensington, London SW7 2BP

Michael Thompson
Department of Chemistry, Birkbeck College, Gordon House, 29 Gordon Square, London WC1 6BT

Katherine Timmins
DQA/TS, The Royal Arsenal East, Woolwich, London SE18 6TD

The use of laser ablation for solid sample introduction has been demonstrated by several groups[1-4] as an alternative to conventional mobilisation methods such as aqueous nebulisation. The performance of the method was satisfactory for certain specific tasks, but fell short of the standard needed for general analysis. It seemed clear that the improvement of laser ablation systems required a study of the fundamental processes involved. The study concentrated on three areas: the ablation process, the form of the ablated material and the transport of that material.

Experimental

The laser used was a ruby-rod type delivering approximately 1 J of energy in both normal and Q-switched mode, which enabled us to control both the number and the peak power of the laser pulses. The laser light was focused on the sample surface in the ablation chamber by using a Zeiss binocular microscope of ×200 or ×500 magnification. The glass ablation chamber had a volume of 18 cm^3. The input and output tubes of the ablation chamber were tangential and there was a window made of a glass microscope cover slip for laser light entry. This is currently the best design devised so far, in terms of sample transport ability and the prevention of "fogging" of the window.

The sample was carried from the chamber by a stream of argon through 5 mm i.d. polythene tubing to an impinger. This device was used to remove material greater than 8 μm in size that might otherwise have dropped out on the way to the ICP torch. A PTFE change-over valve was incorporated into the gas line to allow a change of sample without the entrainment of air. The ICP-AES spectrometer was used with the following conditions: coolant flow, 12 l min^{-1}; auxilary flow, 0.3 l min^{-1}; injector (chamber carrier) flow, 0.5 l min^{-1}, all argon; power, 1.2 kW at 27 MHz; viewing window, a 4-mm square centered at 14 mm above the load coil.

The laser was synchronised with the spectrometer electronics by an optical switch.

The laser ablation events were observed by both still photography and on high-speed cine film. The single shot photographs were taken with a 140 mm lens, 160 ASA colour film and 0.5-s exposure, the exposure starting before and finishing after the event. These were taken both in air and argon. The cine film was shot in colour at a speed of 1000 frames s^{-1}.

The filtration of the aerosol of the ablated material was conducted at various points along the system by means of a 0.4 or 0.8 μm Nucleopore filter in a polythene holder. The form of the ablated material was studied, after coating the filters with gold, by secondary and backscattered electron microscopy. The composition of ablated material was determined using the energy dispersive X-ray analysis system and the size distributions were made automatically on the same system.

The mass loss on ablation was obtained from a piece of copper (weighed to 1×10^{-7} g) before and after the event. The mass of ablated material collected on the filters at given points in the gas line was determined spectrochemically after dissolution of the copper on the filter in nitric acid.

Results

Two processes can be observed when mild steel is ablated by a lightly Q-switched laser in air, a plume of incandescent material and luminous particles flying off at high velocity. If the same material is ablated in an argon atmosphere then the plume is still visible but the particles are not. This suggests that the plume is a plasma and that the particles are burning. Under the same conditions both ceramic materials and zirconium also show plumes. Zirconium gave particularly luminous burning particles in air, and was chosen for the cine photography at a speed of 1000 frames s^{-1}. The cine film was shot with the same conditions as the still photography. The film showed in the first frame (1/1000 s) the production of the plasma plume. The second frame showed the production of particles with a much reduced plasma plume. The third frame showed no plasma plume and no further particles being produced. Subsequent shots only showed particles in flight.

A secondary electron micrograph (Fig. 1) of a cross-section through an ablation crater produced by a lightly Q-switched laser shows a tear-drop shaped crater with a smooth neck and overlapping material, once apparently molten on the surface of the sample. The bottom of the crater is rough with pitting, thus suggesting a different ablation process.

A further secondary electron micrograph (Fig. 2) shows the form of typical ablated material (stainless steel) that reaches the plasma. Most of the particles collected were spherical and

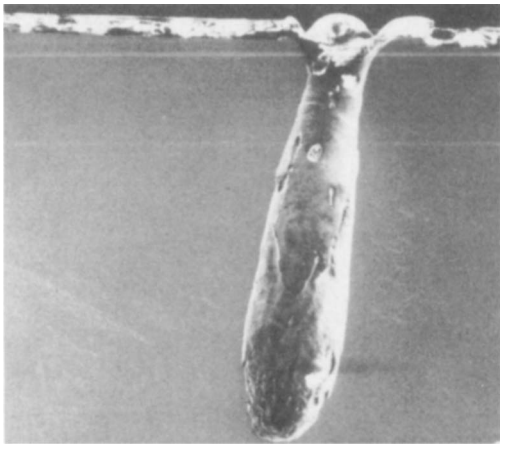

Fig. 1. Cross section through a laser ablation crater in a stainless-steel sample. Depth of crater, 580 μm

almost smooth, with a small amount of amorphous material on the surface. This amorphous material can also be seen on the filter in the background. The spherical particles had evidently been formed directly from the liquid. The amorphous material is thought to be condensate from the plasma plume. The particle size distribution (Fig. 3) of this spherical material shows that a majority of particles are between 0 and 2 μm, but with a tail up to 8 μm. However, the mass distribution shows the 4–6 μm sizes to be most important in terms of instrument response.

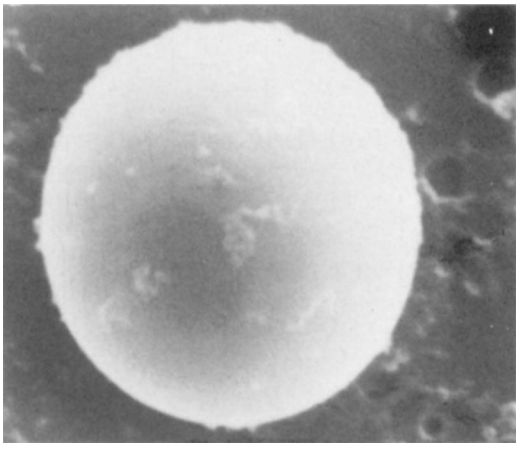

Fig. 2. A sphere of stainless steel produced by laser ablation. Diameter, 3.7 μm

An inspection of material collected in the impinger showed spheres of assorted sizes greater than 1 μm in groups of up to 20, welded together by a meniscus. Thus, the spheres must have been molten when they came into contact or were separating out from a larger droplet. When materials such as ceramic that are more crystalline or brittle are ablated, the finer material leaving the torch is similarly spherical, but larger angular fragments that do not appear to have been melted can be collected from the impinger.

Mass loss experiments with copper showed that at maximum laser power approximately 20 μg were ablated at each shot. However, only 30% of this leaves the chamber (the rest appears as quenched molten material on the chamber walls) and only 5% passes through the torch. Of the material leaving the torch, it is estimated that only 1% of that mass is of a size less than 0.8 μm.

Conclusions

It seems clear that two separate processes contribute to the over-all ablation event and to the material that is eventually analysed. The plasma plume is formed initially from material directly volatilised from the sample surface. This gives rise to the intense emission above the ablation site and to the fine amorphous material that is condensed from the vapour phase. Subsequently, a pool of liquid is formed by interaction of the solid sample with the plasma plume, and this is explosively ejected from the crater to form the spherical particles. This double process has relevance to the question of selective volatilisation, even though the spherical matter predominates in the material that is analysed.

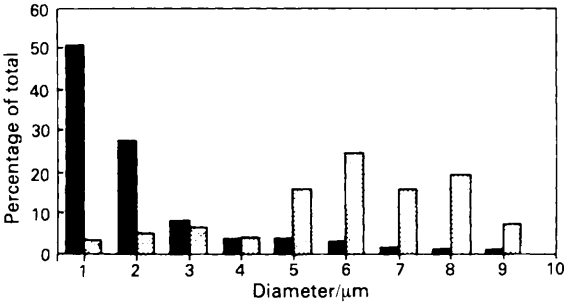

Fig. 3. Particle size distribution and mass distribution of material from the ablation of a stainless-steel sample. The solid blocks represent the number of particles and the dotted blocks the relative mass

Only 30% of the mobilised material leaves the ablation chamber and only a fraction of this reaches the torch for analysis. There is clearly scope for improving the efficiency of the transport process, and possibly some benefit to be gained by separating the condensate from the spherical particles for selective analysis.

References

1. Abercrombie, F. N., Silvester, M. D., Murry, A. D., and Barringer, A. R., *in* Barnes, R. M., *Editor*, "Applications of Inductively Coupled Plasmas to Emission Spectrometry," Franklin Institute Press, Philadelphia, 1978, p. 121.
2. Ishizuka, T., and Uwamino, Y., *Anal. Chem.*, 1980, **52**, 125.
3. Thompson, M., Goulter, J. E., and Sieper, F., *Analyst*, 1981, **106**, 32.
4. Carr, J. W., and Horlick, G., *Spectrochim. Acta, Part B*, 1982, **37**, 1.